Design Guideline - The Internal PI Compensator of an off-line Flyback Converter for USB Power Delivery Applications

Abstract

In order to reduce the external components of an off-line flyback converter for USB Power Delivery applications, an Internal Proportional and Integral Compensator (IPIC) is proposed and integrated into Richtek's Secondary-Side controller (SSC) to provide a regulated output with Constant Voltage (CV) and Constant Current (CC). With the additional phase-boost circuit, the Type-II compensator is resulted to stabilize the flyback converter. This application note provides a comprehensive design guideline to determine specific coefficients of the IPIC and the phase-boost circuit so as to optimize the transient response of a flyback converter for USB PD applications.

Contents

1. Architecture of the Feedback Circuit of the Flyback Converter

Figure 1 shows the architecture of the flyback converter's feedback of the Primary-Side (PS) and the Secondary-Side (SS) in the Richtek's USB PD Controller IC. Both output voltage, V_o, and output current, I_o, of the converter are sensed to the SSC. The internal output voltage feedback signal, V_{vfb}, is obtained from the voltage divider with a ratio determined by $R_{F1}/(R_{F1}+R_{F2})$. The feedback voltage, V_{vfb}, is then compared with the set reference voltage, V_{VREF}, and the voltage error signal, V_{verr} is obtained. Meanwhile the internal output current feedback signal, V_{ifb}, is obtained from the current sensing resistor, R_{CS}, and fed to the Current Sense Amplifier (CSA). The current error signal, Vierr is then obtained by comparing the Vifb with the set reference current, V_{IREF}.

Two diodes are used for the Error Selector to select the dominated control signal, i.e., the higher voltage from V_{verr} or V_{ierr}. The higher one is designated as the dominated error signal, V_{err}. If V_{verr} is selected, the Constant-Voltage (CV) loop of the converter will be regulated. On the other hand, if V_{ierr} is dominated, the Constant-Current (CC) loop will be regulated.

After the error signal, Verr, is compensated by the IPIC, the output of the IPIC, V_c, is buffered and sent out via the OPTO pin to drive the external optocoupler's opto-diode. Through an isolated optocoupler, the compensated signal will be sent to the COMP pin on the Richtek Primary-Side (PS) Controller IC in order to adjust the PWM duty cycle and control the output power of the primary switch.

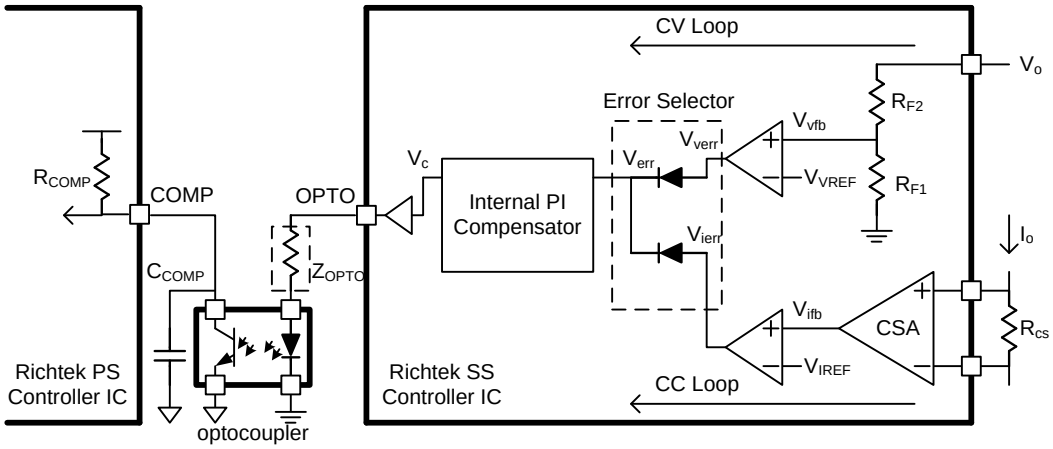

Figure 1. Architecture of the feedback circuit

2. The Transfer Function of Internal PI Compensator, $G_C(s)$

Figure 2(a) shows the block diagram of a typical PI compensator. The output signal, V_c, is processed by the Proportional-Controller (P-Controller) and the Integral-Controller (I-Controller) from the error signal, v_{err}. The PI compensator can be implemented by an Operational Transconductance Amplifier (OTA) consisting of the transconductance, gm, a resistor, R_c, and a capacitor, C_c, as shown in Figure 2(b). As depicted in Fig. 2(b) assuming the OTA has the high output impedance, the transfer function of the IPIC is obtained as follows.

$$G_c(s) = \frac{v_c}{v_{err}} = gm \times R_c + \frac{gm}{s \cdot C_c} = k_P + \frac{k_I}{s} \quad (1)$$

where

$$k_P = gm \times R_c \quad (2)$$

and

$$k_I = \frac{gm}{sC_c} \quad (3)$$

According to Eqs. (2) and (3), one can adjust the control loop's response by tuning the IPIC's parameters, gm, R_C and C_C.

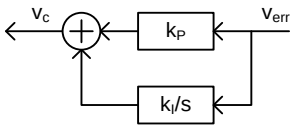

(a). Signal block diagram of the PI compensator

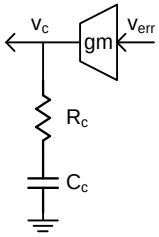

(b). Circuit of the PI Compensator

Figure 2. Internal PI Compensator

In some applications, it is more practical to design the IPIC's parameters in the frequency domain, for that one can rearrange Eq. (1) as the following equation,

$$G_c(s) = gm\left(R_c + \frac{1}{s \cdot C_c}\right) = \frac{gm(s \times R_c C_c + 1)}{s \times C_c} = A_c \frac{\frac{s}{\omega_{zc}} + 1}{s} \quad (4)$$

where

$$A_c = \frac{gm}{C_c} \quad (5)$$

$$\omega_{zc} = 2\pi \times f_{zc} = \frac{1}{R_c C_c} \quad (6)$$

Eq. (4) shows the transfer function of IPIC, Gc(s), has a pole at zero frequency and a zero at f_{zc}. Therefore, the output phase of Gc(s) will be -90° at low frequency and turn to 0° when the input signal's frequency is higher than the IPIC's f_{zc}.

The gain of the IPIC can be further derived as the following equation.

$$|G_c(s)|\Big|_{s=j2\pi f} = \left| A_c \frac{\frac{jf}{f_{zc}} + 1}{j2\pi f} \right| = \frac{A_c}{2\pi} \sqrt{\left(\frac{1}{f_{zc}}\right)^2 + \left(\frac{1}{f}\right)^2} \quad (7)$$

If 1Hz sine wave is injected to the IPIC and f_{zc} is larger than 10Hz, Eq. (7) can be approximated to the following equation.

$$A_{c@1Hz} = |G_c(s)|\Big|_{s=j2\pi} \sim \frac{A_c}{2\pi} = \frac{gm}{2\pi \times C_c} \quad (8)$$

If the input signal's frequency is higher than f_{zc}, Eq. (7) can be simplified to

$$A_{c@HF} = |G_c(s)|\Big|_{s>j2\pi 10f_{zc}} \sim \frac{A_c}{2\pi f_{zc}} = gm \times R_c \quad (9)$$

With given gm, R_c and C_c, the f_{zc}, $A_{c@1Hz}$ and $A_{c@HF}$ are known. Thus, the frequency response of the IPIC can be determined by the Bode diagram as shown in Figure 3.

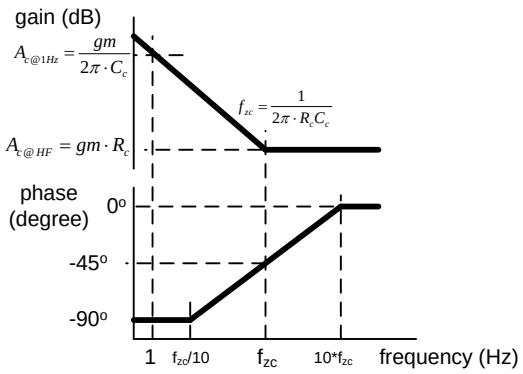

Figure 3. Typical frequency response of the IPIC

Take an example of the designed IPIC with gm = 20μA/V, R_C = 10kΩ and Cc = 33nF. The correspondent f_{zc}, $A_{c@1Hz}$ and $A_{c@HF}$ can be calculated according to Eqs. (6), (8) and (9), respectively.

$$f_{zc} = \frac{1}{2\pi \cdot 10\times10^{3} \cdot 33\times10^{-9}} = 482.3Hz$$

$$A_{c@1Hz} = \frac{20\times10^{-6}}{2\pi \cdot 33\times10^{-9}} = 96.5 = 39.7dB$$

$$A_{c@HF} = 20\times10^{-6} \cdot 10\times10^{3} = 0.2 = -14.0dB$$

Figure 4 shows the calculated frequency response analysis results.

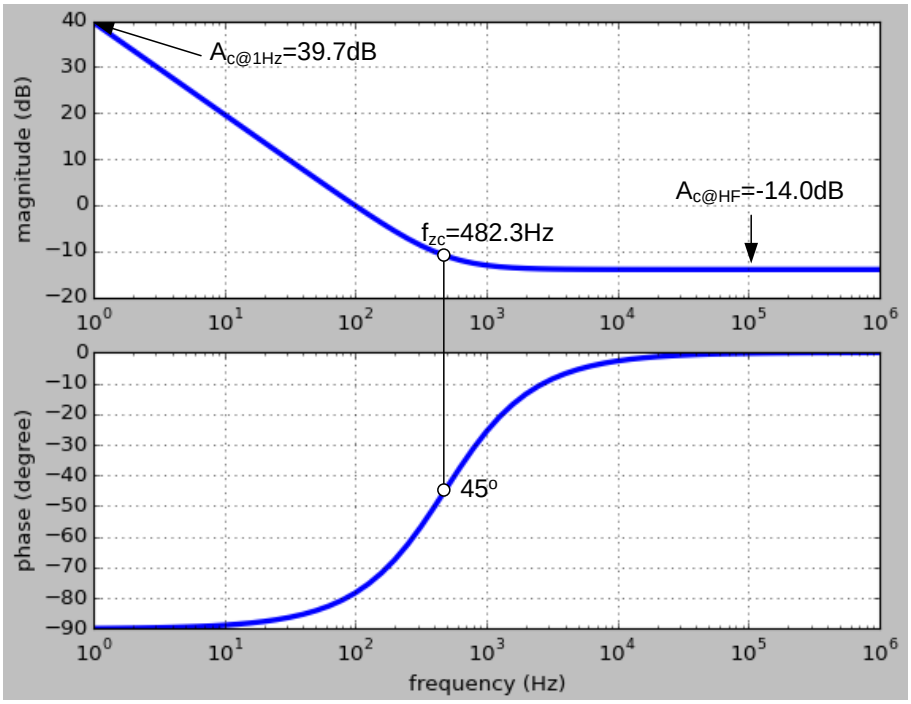

Figure 4. Frequency response of the designed IPIC with gm = 20μA/V, R_C = 10kΩ and C_C = 33nF

According to Eq. (4) and above analysis, the behavior of the IPIC's frequency response can be adjusted by the coefficients, gm, C_C and R_C illustrated in Figure 5. Furthermore by using Eqs. (8) and (9), the IPIC's gain, Ac, can be approximate by $A_{c@1Hz}$ at low frequency and $A_{c@HF}$ at high frequency, respectively. The $A_{c@1Hz}$ is proportional to gm and the inverse of C_C, while the $A_{c@HF}$ is proportional to gm and R_C. Hence, if gm is increased, both the gains $Ac_{@1Hz}$ and $Ac_{@HF}$ of the IPIC's frequency response at low and high frequency are increased as illustrated in Figure 5(a). However, as Cc is increased, the IPIC's gain at low frequency, $A_{c@1Hz}$, is decreased and the zero frequency, f_{zc}, is moved to the lower frequency as illustrated in Figure 5(b). If R_C is increased, f_{zc}, is moved to the lower frequency while $A_{c@HF}$ is increased.

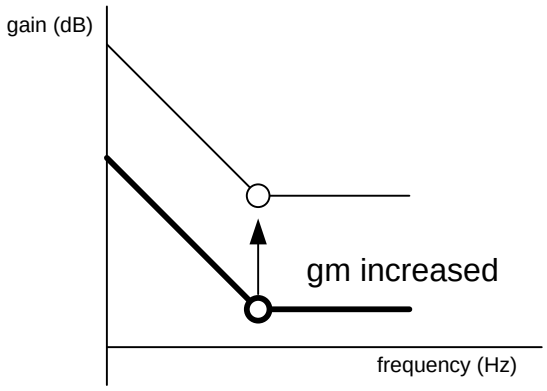

(a)

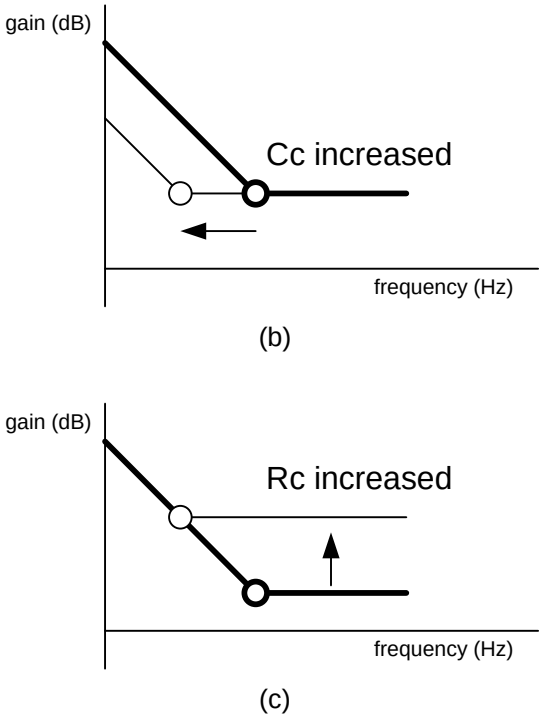

Figure 5. Behavior of the frequency response IPIC according to the change of (a) gm, (b) C_c and (c) R_c

3. The Transfer Function from OPTO to COMP, $G_{OPTO}(s)$

As shown in Figure 1, once the IPIC's transfer function and the frequency response are defined, the feedback circuit transfer function from the node OPTO at the secondary side of the transformer to the node COMP at the primary side of the transformer can be analyzed, where the OPTO and COMP nodes are isolated by the optocoupler. Figure 6 shows the small-signal model of the signal path from OPTO to COMP, which consists an optocoupler, the optocoupler's current-clamping impedance, Z_{OPTO}, and the optocoupler's output low-pass filter formed by R_{COMP} and C_{COMP}. Note that the R_{COMP} is a built-in component in the PS Controller IC, while the C_{COMP} is the combination of the external capacitor and the parasitic capacitor of the optocoupler. The optocoupler can therefore be modeled as the Current-Control Current Source (CCCS) with the gain specified as the Current-Transfer Ratio (CTR). With that the transfer function of the voltage from the node OPTO to the node COMP is derived as Eq. (10).

$$G_{OPTO}(s) = \frac{v_{COMP}(s)}{v_{OPTO}(s)} = CTR \times \frac{R_{COMP}}{Z_{OPTO}} \times \frac{1}{sR_{COMP}C_{COMP}+1} = A_{OPTO}\frac{1}{s/\omega_{pOPTO}+1} \quad (10)$$

where

$$\omega_{pOPTO} = 2\pi \times f_{pOPTO} = \frac{1}{R_{COMP}C_{COMP}} \quad (11)$$

$$A_{OPTO} = CTR \times \frac{R_{COMP}}{Z_{OPTO}} \quad (12)$$

From Eq. 10, $G_{OPTO}(s)$ is a low-pass filter whose pole is located at ω_{pOPTO} if Z_{OPTO} is a resistor. The DC gain of $G_{OPTO}(s)$ can be adjusted by the ratio of R_{COMP} and Z_{OPTO}.

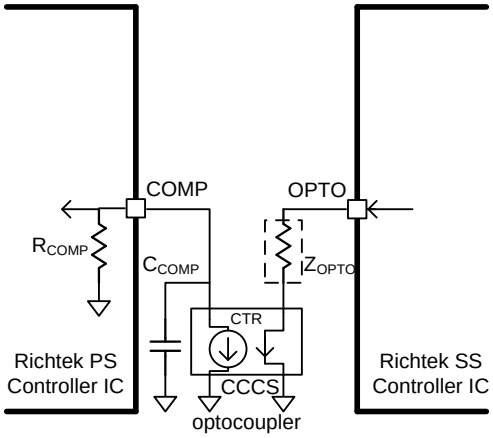

Figure 6. Small-signal model of the optocoupler

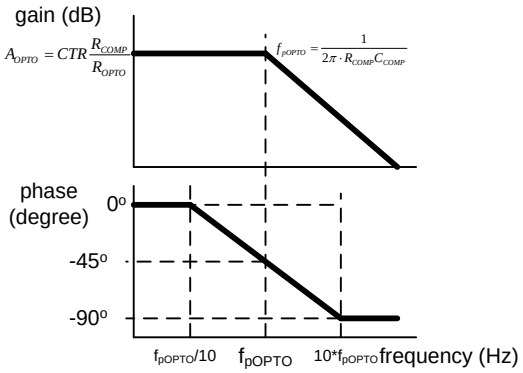

Figure 7. Typical frequency response of $G_{OPTO}(s)$ without the phase-boost circuit

Figure 7 illustrates typical frequency response of $G_{OPTO(S)}$, for example if the parameters are chosen for a Z_{OPTO} = R_{OPTO} = 200Ω, CTR = 0.5, R_{COMP} = 20kΩ and C_{COMP} = 10nF, the frequency response is illustrated in Figure 8.

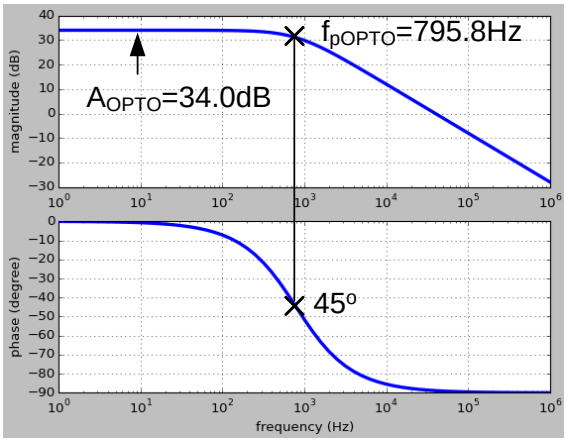

Figure 8. Frequency response of $G_{OPTO}(s)$ with R_{OPTO} = 200Ω, CTR = 0.5, RCOMP = 20kΩ and C_{COMP} = 10nF

The pole in this example is at 789.8Hz, which is within the loop's bandwidth. When ωp_{OPTO} is too low and the bandwidth of the loop response will be limited by this pole. As illustrated in Figure 9 the current-clamping impedance, Z_{OPTO}, can be further configured as the so-called phase-boost circuit with the additional R_{PBOPTO} and C_{PBOPTO} in parallel with R_{OPTO}. The admittance of $G_{OPTO(s)}$ can be derived as the following equation which has a zero, ωz_{PBOPTO}, at the low frequency and a pole, ωp_{PBOPTO}, at the high frequency.

$$\frac{1}{Z_{OPTO}(s)} = \frac{i_{OPTO}(s)}{v_{OPTO}(s)} = \frac{1}{R_{OPTO} \,||\, \left(R_{PBOPTO} + \frac{1}{sC_{PBOPTO}}\right)}$$

$$= \frac{1}{R_{OPTO}} \times \frac{s(R_{OPTO} + R_{OPTO1})C_{OPTO1}+1}{sR_{PBOPTO}C_{PBOPTO}+1} = \frac{1}{R_{OPTO}} \times \frac{s/\omega_{zPBOPTO}+1}{s/\omega_{pPBOPTO}+1} \quad (13)$$

$$\omega_{pPBOPTO} = 2\pi \times f_{pPBOPTO} = \frac{1}{R_{PBOPTO}C_{PBOPTO}} \quad (14)$$

$$\omega_{zPBOPTO} = 2\pi \times f_{zPBOPTO} = \frac{1}{(R_{OPTO}+R_{PBOPTO})C_{PBOPTO}} \quad (15)$$

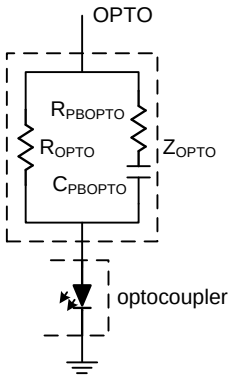

Figure 9. Phase-boost circuit of Z_{OPTO}

From Eq. (14) and (15), ωz_{PBOPTO} has lower frequency than ωp_{PBOPTO} due to the additional R_{OPTO} at the denominator. Since the phase of $G_{OPTO}(s)$ will be increased at $\omega_{pPBOPTO}$, and then decreased at $\omega_{pPBOPTO}$, the phase can be boosted is between the frequency, $\omega_{pPBOPTO}$ to $\omega_{pPBOPTO}$. The transfer function $G_{OPTO}(s)$ can be expressed as Eq. (18) when in terms of the phase-boost circuit.

$$G_{OPTO}(s) = \frac{v_{COMP}(s)}{v_{OPTO}(s)} = A_{OPTO} \times \frac{1}{s/\omega_{pOPTO}+1} \times \frac{s/\omega_{zPBOPTO}+1}{s/\omega_{pPBOPTO}+1} \quad (16)$$

where

$$A_{OPTO} = CTR \times \frac{R_{COMP}}{R_{OPTO}}$$

Note that one can use ωz_{PBOPTO} to cancel ωp_{OPTO} and leave the ωp_{PBOPTO} to determine the -3dB frequency of $G_{OPTO}(s)$. Rearange Eq. (14) to get C_{PBOPTO} for a given ωp_{PBOPTO},

$$C_{PBOPTO} = \frac{1}{\omega_{pPBOPTO} \times R_{PBOPTO}} \quad (17)$$

Let $\omega p_{OPTO} = \omega p_{PBOPTO}$,

$$\frac{1}{\omega_{pOPTO}} = (R_{OPTO}+R_{PBOPTO})C_{PBOPTO} \quad (18)$$

After substitution,

$$\frac{1}{\omega_{pOPTO}} = (R_{OPTO} + R_{PBOPTO})\frac{1}{\omega_{pPBOPTO} \times R_{PBOPTO}} = \left(\frac{R_{OPTO}}{R_{PBOPTO}}+1\right)\frac{1}{\omega_{pPBOPTO}} \quad (19)$$

Rearrange

$$R_{PBOPTO} = \frac{R_{OPTO}}{\frac{\omega_{pPBOPTO}}{\omega_{pOPTO}}-1} \quad (20)$$

From above equations, the original pole of $G_{OPTO}(s)$, ωp_{OPTO}, is cancelled by the designed ωz_{PBOPTO} and moved to the desired pole, ωp_{PBOPTO}. Thus, the bandwidth limited by the original pole of $G_{OPTO}(s)$ can be extended by the adjustment of the phase-boost circuits' R_{PBOPTO} and C_{PBOPTO} according to the ratio of the desired and the original pole frequency from Eq. (20).

As illustrated in the example of Figure 8, the pole, f_{pOPTO}, of $G_{OPTO}(s)$ without the phase-boost circuit is located at 795.8Hz, which is too low and will affect the response of the flyback converter. Therefore, we need to add the phase-boost circuit to shift f_{pOPTO} to a 10 times frequency :

$\omega p_{PBOPTO} = 10 \times \omega p_{OPTO}$

According to Eq. (20),

$$R_{OPTO1} = \frac{R_{OPTO}}{\frac{\omega_{pPBOPTO}}{\omega_{pOPTO}}-1} = \frac{200\Omega}{10-1} = 22.2\Omega$$

And Eq. (17),

$$C_{OPTO1} = \frac{1}{\omega_{pPBOPTO} \times R_{OPTO1}} = \frac{1}{2\pi \times 10 \times 795.8Hz \times 22.2\Omega} = 900nF$$

After obtaining R_{PBOPTO} and C_{PBOPTO}, the phase-boost circuit's pole and zero from Eq. (14) and (15) are obtained as following frequencies,

$$f_{pPBOPTO} = \frac{1}{2\pi \times R_{PBOPTO}C_{PBOPTO}} = \frac{1}{2\pi \times 22.2\Omega \times 900nF} = 7.96KHz$$

$$f_{zPBOPTO} = \frac{1}{2\pi \times (R_{PBOPTO} + R_{PBOPTO})C_{PBOPTO}} = \frac{1}{2\pi \times (200\Omega + 22.2\Omega) \times 900nF} = 795.8Hz$$

To be noted, $f_{zPBOPTO}$ is 795.8Hz, which is the same as f_{pOPTO}. Thus, the original pole is cancelled by the phase-boost circuit. The designed phase-boost circuit's frequency response is illustrated in Figure 10.

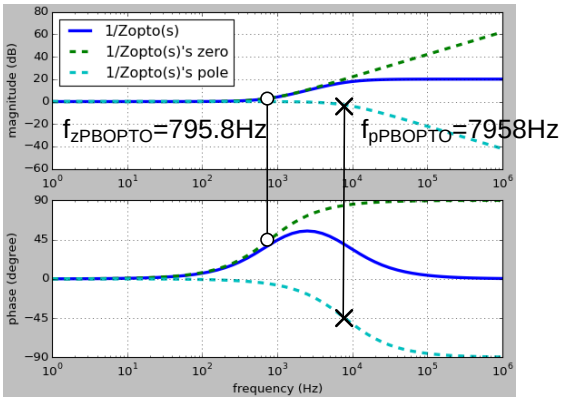

Figure 10. Frequency response of the phase-boost circuit

The following example shows the resulted phase-boost $G_{OPTO}(s)$. As shown in Figure 11, in comparison with $G_{OPTO}(s)$ without phase-boost, the pole is shifted as expected to 10 times original frequency from around 800Hz to around 8KHz

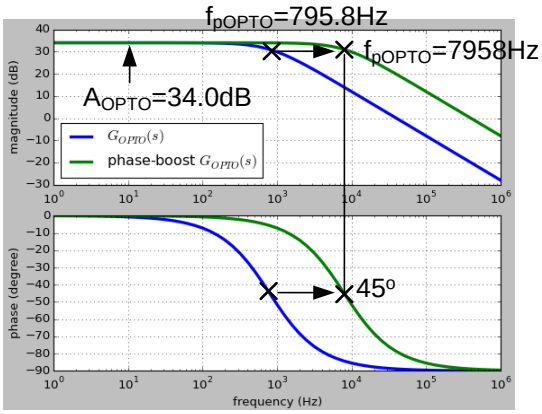

Figure 11. Frequency response of the phase-boost $G_{OPTO}(s)$ compensated with R_{PBOPTO} = 22.2Ω and C_{PBOPTO} = 200nF compared to the original one with R_{OPTO} = 200Ω, CTR = 0.5, R_{COMP} = 20KΩ and C_{COMP} = 10nF

4. The Transfer Function of Feedback Circuit, $G_{CV}(s)$ and $G_{CC}(s)$

The small signal model of the feedback circuit as shown in Figure 12 depends on either CV or CC feedback loop illustrated by Figure 12(a) and (b), respectively. The buffer gain from the output of IPIC to the OPTO node is simplified as 1.

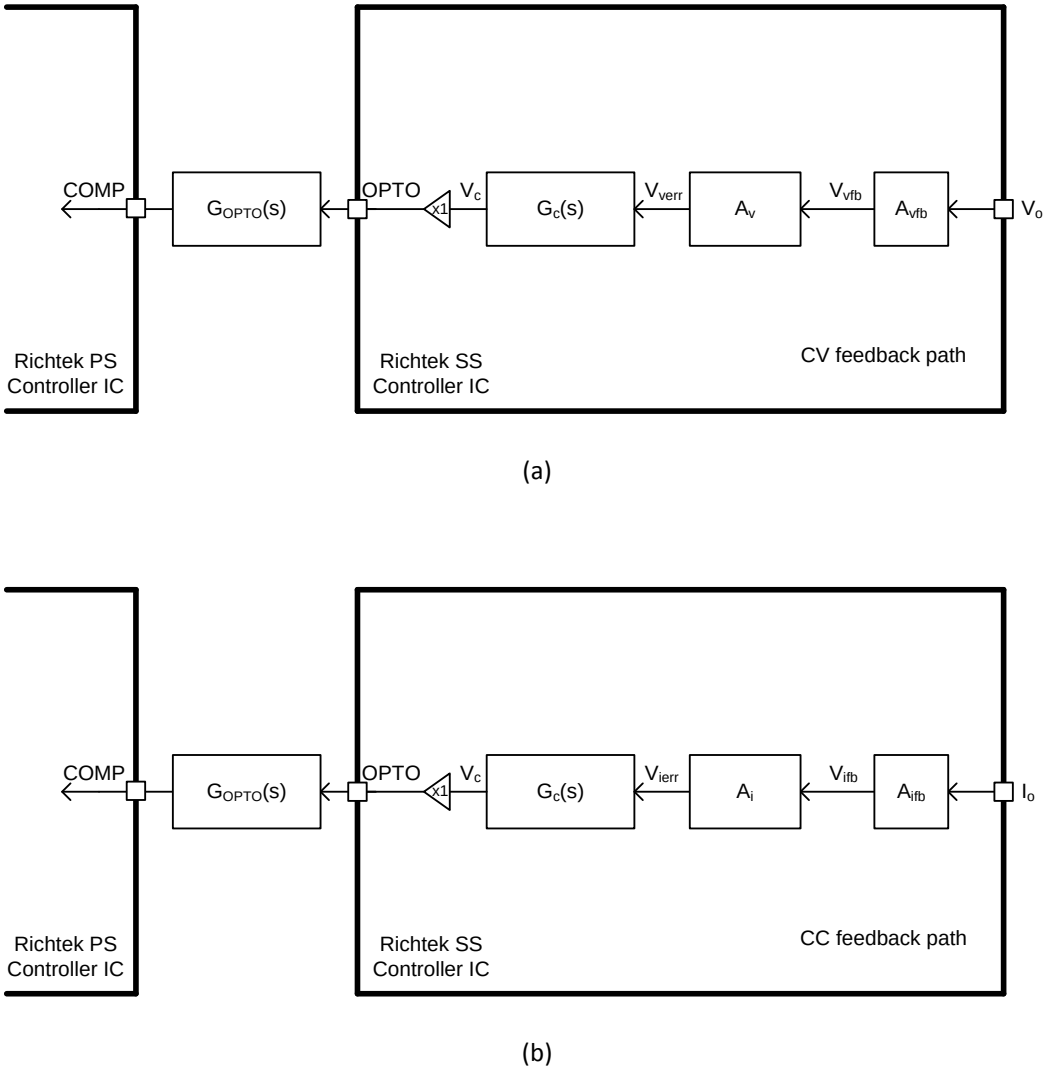

Figure 12. Small signal transfer function of feedback circuit with (a) CV feedback path, and (b) CC feedback path

The transfer function for CV and CC feedback path are defined as follows.

$$G_{CV}(s) = A_v A_{vfb} G_{OPTO}(s) G_c(s) \quad (21)$$

$$G_{CC}(s) = A_i A_{ifb} G_{OPTO}(s) G_c(s) \quad (22)$$

Assuming the IPIC uses the same coefficients for both the CV and CC feedback path except different gains, once the CV feedback path is designed, the CC feedback path will share the same pole and zero position. By adjusting the CC feedback path's gain to be less than CV's, the bandwidth of the CC loop will be less than that of the CV loop. Thus, one shall firstly focus on defining the CV feedback path transfer function.

Expand Eq. (21).

$$G_{CV}(s) = A_v A_{vfb} A_{OPTO} \times \frac{1}{\frac{s}{\omega_{pOPTO}}+1} \times \frac{\frac{s}{\omega_{zPBOPTO}}+1}{\frac{s}{\omega_{pPBOPTO}}+1} A_{cmp} \frac{\frac{s}{\omega_{zcmp}}+1}{s} \quad (23)$$

If the optocoupler's pole is cancelled by the phase-boost circuit, Eq. (23) could be further simplified to the following equation.

$$G_{CV}(s) = A_v A_{vfb} A_{OPTO} A_{cmp} \frac{1}{\frac{s}{\omega_{pPBOPTO}}+1} \frac{\frac{s}{\omega_{zcmp}}+1}{s} = A_{CV} \times \frac{1}{\frac{s}{\omega_{pPBOPTO}}+1} \frac{\frac{s}{\omega_{zcmp}}+1}{s} \quad (24)$$

The transfer function, Eq. (24), reduces to one zero and two poles, so-called Type-II compensator. Figure 13 shows the typical frequency response of the compensated CV feedback path. The designer can determine the frequency respone by well programming the IPIC's gm, R_c, and C_c and the phase-boost circuits R_{PBOPTO} and C_{PBOPTO}.

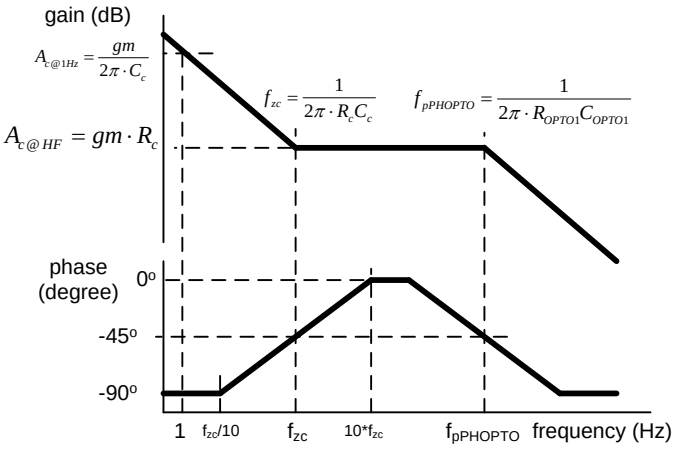

Figure 13. Frequency response of the CV feedback path

A typical peak-current mode flyback converter's power stage has a pole which is determined by its output capacitance and the loading resistance. The zero of the IPIC, ω_{zcmp}, is programmed to compensate the pole of the flyback converter's power stage. The pole of the phase-boost circuit, $\omega_{pPBOPTO}$, is typically designed at 1 to 10KHz depending on the converter's bandwidth. The middle gain, A_{CV}, can be designed to have enough phase-margin.

By using parameters as in previous examples, the IPIC's parameters are gm = 20μA/V, R_c = 10kΩ and C_c = 33nF and the optocoupler is biased with R_{OPTO} = 200Ω which results in CTR = 0.5. The COMP node has R_{COMP} = 20kΩ and C_{COMP} = 10nF. The pole created by R_{COMP} and C_{COMP} is cancelled via the zero designed by the phase-boost circuit, R_{PBOPTO} = 22.2Ω and C_{PBOPTO} = 900nF.

The green line in Figure 14 shows the frequency response of $G_{CV}(s)$ with the phase-boost circuit. The zero is determined by the IPIC while the 2nd pole is determined by the phase-boost circuit. The cut-off frequency at 0dB of the phase-boost $G_{CV}(s)$ in comparison with the one without phase-boost circuit, is extended.

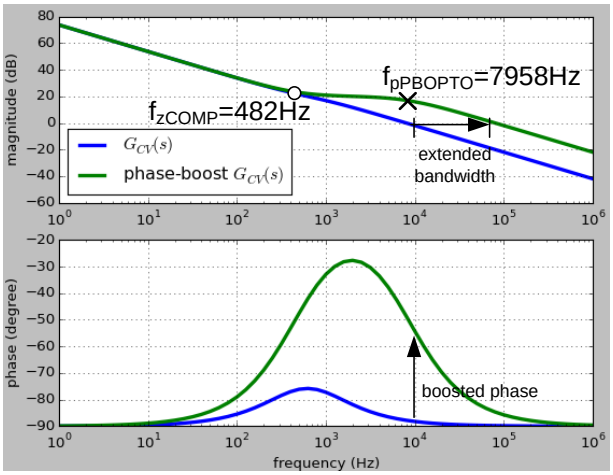

Figure 14. Frequency response of the compensated CV feedback path without (blue line) and with (green line) the phase-boost circuit

5. Conclusion

The Richtek IPIC is demonstrated with the phase-boost circuit providing a Type-II compensator so as to stabilize a flyback converter. It is guided by the transfer equations, gain, zero and pole of the Type-II compensator can be free determined by the designer to optimize the transient response of different flyback converters under different operating conditions.

Next Steps	
Richtek Newsletter	Subscribe Richtek Newsletter

Richtek Technology Corporation
14F, No. 8, Tai Yuen 1st Street, Chupei City
Hsinchu, Taiwan, R.O.C.
Tel: 886-3-5526789